Journal of
Proteomics & Bioinformatics

Madoz-Gúrpide et al., J Proteomics Bioinform 2016, 9:6
DOI: 10.4172/jpb.1000403

Research Article Open Access

Proteomic Profiling of Ewing Sarcoma Reveals a Role for TRAF6 in Proliferation and Ribonucleoproteins/RNA Processing

Juan Madoz-Gúrpide[1*], David Herrero-Martín[2], Gonzalo Gómez-López[3], Lourdes Hontecillas-Prieto[4], Michele Biscuola[4], Cristina Chamizo[1], Daniel García-Domínguez[4], David Marcilla[4], Ana Teresa Amaral[4], José Luis Ordóñez[5] and Enrique de Álava[4*]

[1]*Cancer Biomarkers Research Group, Health Research Institute Fundación Jiménez Díaz (IIS-FJD), UAM, Madrid, Spain*
[2]*Sarcoma Research Group, Bellvitge Biomedical Research Institute, Barcelona, Spain*
[3]*Bioinformatics Unit, Spanish National Cancer Research Centre (CNIO), Madrid, Spain*
[4]*Pathology Unit, Instituto de Biomedicina de Sevilla (IBiS), Hospital Universitario Virgen del Rocío/CSIC/Universidad de Sevilla, Seville, Spain*
[5]*Molecular Cytogenetics, Centro de Investigación del Cáncer-IBMCC, Universidad de Salamanca-CSIC, Salamanca, Spain*

Abstract

Notwithstanding advances over the last decade in the comprehension of the molecular biology of Ewing sarcoma (ES), we still lack an understanding of critical issues, especially those regarding its genesis. In particular, little effort has been devoted to characterization of the proteic component of the mechanisms and pathways deployed by the activation of the fusion protein resulting from chromosomal translocation. We decided to investigate the proteic alterations of an ES cell line bearing a representative fusion protein. The combination of RNA interference of EWS-FLI1 in the ES cell line TC-71, a proteomic analysis by 2-D electrophoresis and subsequent mass-spectrometry identification, and a global overrepresentation study detected changes in more than 500 spots. Forty-three proteins were identified as being significantly differentially abundant. As expected, we found and validated changes in proteins linked to nucleotide processing, transcription regulation, ribonucleoproteins, helicases, cell-cycle control and proliferation, and metabolic processes. Additionally, TNF receptor-associated factor 6 was revealed as a hub node. Our strategy showed the potential to reveal the protein interplay associated with the known functions of the fusion protein: binding to DNA and RNA in order to act as aberrant transcription factors or potent repressors, or by altering RNA processing.

Keywords: Comparative proteomics; Ewing sarcoma; Molecular pathogenesis; Two-dimensional gel electrophoresis

Introduction

Ewing sarcoma (ES) is a high-grade malignancy in which approximately 75% of cases are localized at diagnosis, and 25% are initially metastatic [1,2]. Refractory and/or recurrent ES remains a clinical challenge because the disease's resistance to therapy makes it difficult to achieve long-lasting results. There is an urgent need to improve cure rates for localized, metastatic, and recurrent disease while decreasing treatment-related morbidity. The general treatment paradigm for localized ES is relies on a multidisciplinary approach, coupling chemotherapy with cyclic combinations of locoregional management consisting of surgery with or without radiation treatment [3]. Different combinations of drugs involving doxorubicin, vincristine, cyclophosphamide, ifosfamide, etoposide, and dactinomycin have been employed in consecutive first-line trials, with the aim of tailoring therapies to the individual molecular profile of the patients. However, the current overall disease-free survival rate for metastatic disease is 25%. For long-term survivors of childhood ES (defined as patients that survived ≥ 5 years as of diagnosis) with localized disease the overall reported mortality is 25%. Disease recurrence/progression accounts for 60% of deaths. These data indicate the limitations of conventional cytotoxic chemotherapy and underscore the need for novel targeted therapies in ES, reflecting the current knowledge into the biology of the EWS-FLI1 protein in the initiation and progression of ES.

ES is a malignant tumor that develops in the bone or in soft tissue of children and young adults. Although its incidence is approximately 3 cases per 1 million per year, it is the second most frequent primary malignant bone tumor in childhood and adolescence after osteosarcoma. It is more common in males and can occur anywhere in the body, but is mostly found in the long bones and pelvis; in about 10% of cases, ES is extraskeletal [4].

ES is characterized by the presence of specific balanced chromosomal translocations, the most frequent being t(11;22)(q24;q12), which invariably fuses the 5' region of the *Ewing sarcoma breakpoint region 1* locus (*EWSR1*) with the 3' region of one of several members of the ETS family of transcription factors. The resulting fusion is translated into a chimeric protein linking the NH2-terminal domain of the RNA-binding protein EWS with the DNA-binding portion of a given ETS transcription factor, FLI1, in 90% of cases [5-8]. EWS-FLI1 acts as an aberrant transcription factor [9] both as a transcriptional activator and repressor of similarly sized sets of target proteins, including transcription, apoptotic, or signal transduction factors [10-12]. There is strong evidence for the oncogenic potential of EWS-ETS fusions [7]. In addition to the chimeric protein itself, the cellular context also contributes to the phenotype, as it has been extensively reported that the introduction of EWS-ETS fusions into different cell models resulted in diverse outcomes, ranging from the induction of cell-cycle arrest, or apoptosis, to dedifferentiation [13-17].

***Corresponding authors:** Juan Madoz-Gúrpide, Cancer Biomarkers Research Group, IIS-Fundación Jiménez Díaz, UAM, Avda. Reyes Católicos 2, E-28040, Madrid, Spain, Tel: +34-915504804; E-mail: JMadoz@fjd.es

Enrique de Álava, Pathology Unit, Instituto de Biomedicina de Sevilla (IBiS), Hospital Universitario Virgen del Rocío/CSIC/Universidad de Sevilla, Avda. Manuel Siurot s/n, E-41013, Seville, Spain, Tel: +34- 955923089; E-mail: enrique.alava.sspa@juntadeandalucia.es

Received May 18, 2016; **Accepted** June 23, 2016; **Published** June 27, 2016

Citation: Madoz-Gúrpide J, Herrero-Martín D, Gómez-López G, Hontecillas-Prieto L, Biscuola M, et al. (2016) Proteomic Profiling of Ewing Sarcoma Reveals a Role for TRAF6 in Proliferation and Ribonucleoproteins/RNA Processing. J Proteomics Bioinform 9: 166-175. doi:10.4172/jpb.1000403

Although substantial evidence suggests that genetic abnormalities play a primary function in the development of tumors, there is also ample proof that aberrations in cancer can occur through changes in the phenotype that arise in the absence of alterations in the DNA sequence, and that many such phenotypic changes are directly related to proteins, some examples of which include splice variation, time-dependent changes in abundance levels, cellular location, turnover number, alterations in signaling pathways, interactions, post-translational modifications such as phosphorylation, glycosylation, acetylation, etc., and degradation processes; these processes are aberrantly regulated in many types of cancers and cannot be predicted by DNA sequencing or measurement of mRNA expression. In fact, it has become evident that there is considerable discrepancy between mRNA and protein translation [18]. Assuming the classical paradigm that proteins are the cell's ultimate tools, its *de facto* effectors, and given that the majority of treatments with antitumor drugs are directed against specific proteins, we considered the potential advantages of monitoring protein abundance in a global manner in an effort to gain a better understanding of the underlying biology of ES.

We developed a stable RNA interference model by knocking down EWS-FLI1 in the ES cell line TC-71 [19], so we can analyze in depth, using proteomic approaches, the alterations in the landscape of proteins influenced by the chimeric protein. By inquiring on the differences between specific experimental conditions and using highly sensitive techniques as the final readout, we were able to typify the differences in protein abundance that were associated with the expression/repression of EWS-FLI1. Using two-dimensional gel electrophoresis (2D-PAGE) and mass spectrometry (MS), we performed a comparative global protein abundance study of the TC-71 with shEWS-FLI1. Our shEWS-FLI1 model unveiled a primary dynamic play of proteins involved in different aspects of nucleotide processing, from changes in histone levels wrapping the chromatin in the nucleosome, DNA unwinding through helicases, RNA binding and splicing, RNA elongation from polymerases and aminoacyl tRNA ligases, to transcription initiation from transcription factors. All these modulations are suggestive of an internal cellular program of transcriptional misregulation in cancer. In addition, other changes in protein expression point to alterations in diverse metabolic pathways, which might be indicative of disruption of energetic fueling and consumption.

Materials and Methods

Cell lines and shRNAi interference

A-4573, A-673, CADO-ES, RD-ES, RM82, SK-ES-1, SK-N-MC, STA-ET-1, STA-ET-2.1, STA-ET-10, TC-32, TC-71, TTC-466, VH-64, and WE-68 ES cell lines, as well as MCF7 (breast) and PC-3 (prostate) cell lines were obtained and maintained as previously described [20]. shEWS-FLI1 construction was performed as described earlier [19]. Briefly, shRNAi sequences were designed to target the fusion point between EWS and FLI1, and the resulting insert was sequenced and then transfected into TC-71 cells, which were finally selected for positive clones. RNA interference was monitored by analyzing EWS-FLI1 protein and mRNA levels using Western blotting (WB) and qRT-PCR, respectively. Up to 40 clones were analyzed at both early and late stages (8 cellular passages later).

Two-dimensional gel electrophoresis

Cell culture plates were washed 3 times with 10 ml of ice-cold PBS. Next, lysates were obtained by scraping cells into 200 µl of ice-cold lysis buffer containing 8 M urea, 2 M thiourea, 4% (w/v) CHAPS and protease inhibitor cocktail (Roche). Proteins were precipitated with the 2-D Clean-Up Kit (GE Healthcare) to remove salts and impurities and were resuspended in lysis buffer. Total protein (150 µg, estimated using the 2-D Quant Kit (GE Healthcare)) was prepared in 350 µl of rehydratation solution (8 M urea, 2% (w/v) CHAPS, 0.5% (w/v) DTT, 0.75% (v/v) IPG buffer and 0.002% bromophenol blue), and subsequently, IPG strips (18 cm, pH 3-11 non-linear Immobiline DryStrip gels, GE Healthcare) were rehydrated overnight with the sample/rehydration buffer mixture. Isoelectrofocusing for the first-dimensional separation was performed in an Ettan IPGphor 3 apparatus (GE Healthcare) for 50,000 Vh at high voltages and 20°C. Reduction and alkylation were accomplished by equilibration of the strips in buffer I containing 6 M urea, 2% SDS, 375 mM Tris-HCL (pH 8.8), 20% glycerol, and 2% (w/v) DTT, and buffer II containing 6 M urea, 2% SDS, 375 mM Tris-HCL (pH 8.8), 20% glycerol and 2.5% (w/v) iodoacetamide. Next, the gel strips were electrophoresed in vertical 12% SDS-PAGE gels for the second dimension, using a Protean II XL Cell (Bio-Rad), under a constant power of 17 W/gel.

Image analysis of 2-D protein spots

Silver staining (Silver Staining Kit, GE Healthcare) according to a modified protocol (without glutaraldehyde fixation solution) was used to detect protein spots and perform image analysis. Subsequently, synthetic gels were constructed, and the resultant protein patterns were qualitatively and quantitatively analyzed by Melanie 5 software (GeneBio). For subsequent MS analysis, preparative 2-D gels were run in parallel and stained with Sypro Ruby (Sigma-Aldrich), which does not interfere with the technique. All samples were run in sextuplicate.

MS analysis

All proteins were processed and analyzed for their identification in the Genomics and Proteomics Unit of the Centro de Investigación del Cáncer of Salamanca. Differentially abundant protein spots were manually excised from the gels, digested with trypsin, and processed for MALDI-ToF MS analysis in a AutoFlex system (Bruker Daltonics) in a positive ion reflector mode. The ion acceleration voltage was 20 kV. Each spectrum was internally calibrated with the masses of two trypsin autolysis products. For protein identification by matching peptide-mass fingerprinting, the tryptic peptide mass maps were transferred through MS BioTools™ program (Bruker Daltonics) as inputs to search the Swiss-Prot non-redundant human database (minimal score change cut-off was set to 54; $p<0.05$) using MASCOT software (Matrix Science). Fully-tryptic digestion with up to one missed tryptic cleavage were considered, a mass accuracy of 100 ppm, and 0.8 Da mass tolerances for precursor and product ions were used for all the tryptic-mass searches. Carbamidomethylation of cysteines, variable oxidation of methionine and N-terminal acetylation were considered. Peptides having MASCOT scores below a significant threshold (5%) were not considered for analysis. One percent false discovery rate using the Percolator was used for peptide validation [21]. Only proteins with at least two significant peptides were considered for analysis.

Bioinformatic analyses

We performed functional profiling of the proteomic data using the FatiGO tool from the Babelomics server [22]. Functional enrichment analysis of overrepresented ontology terms allowed us to categorize by Gene Ontology (GO) the molecular function, biological process, and cellular localization of the unique proteins identified in this study. Likewise, overrepresentation analysis of pathways was launched against the Biocarta, KEGG, and Reactome databases, in order to find the

pathways of relevance in which the annotated proteins on our list were strongly enriched. Finally, we searched for enrichment in regulatory elements within our list of protein IDs, thus analyzing both miRNA databases in search of miRNA targets, and transcription factor binding-site databases (Jaspar TFBS). In all the cases, only those terms showing FDR <0.05 were considered statistically significant.

Gene expression analysis by quantitative real-time PCR

Total RNA from cell lines was isolated using the RNeasy FFPE kit (Qiagen). cDNA was produced using the Universal Transcriptor cDNA synthesis kit (Roche Diagnostics, Spain) according to the manufacturer's recommendations for random hexamer primer. The levels of *PA2G4, PPIB, PRDX6*, and *TRAF6* gene expression were determined using a quantitative real-time PCR assay using *ATP5E* as a housekeeping gene. Primers were designed based on the sequences from GeneBank listed in Table S1. qPCR assays were performed using the LightCycler480 II system (Roche Applied Science, Switzerland) for 45 cycles with the sets of specific primers described in Table S1 (Figure S1). *PA2G4, PPIB, PRDX6*, and *TRAF6* expression levels were normalized to the calibrator levels (IMR90 fibroblast human cell line) and compared to hMSC (mesenchymal stem cells) from healthy donors recruited from the Salamanca University Hospital.

Immunohistochemistry (IHC)

Sections (5 μm) from formalin-fixed, paraffin-embedded (FFPE) ES tissue samples were stained with hematoxylin and eosin. Representative malignant areas were carefully selected from the stained sections of each tumor, and 21-mm diameter tissue cores were obtained from each specimen. IHC was carried out on sequential tissue microarray sections by the Envision method (Dako, Denmark) using the following primary antibodies: PA2G4, PRDX6 and TRAF6. Three tissue microarrays, including 42 ES samples available from the HUVR Biobank, were used to validate biomarker abundance. Only those tumor cells evaluated as clearly stained were considered to be positive. The IHC results were evaluated by 2 pathologists (E.A. and D.M.), who scored the average abundance of markers in duplicate samples.

WB analysis

WB assays were performed as described earlier [20]. Protein abundance was determined using the following antibodies: anti-PA2G4 (Sigma-Aldrich HPA016484); anti-PRDX6 (Sigma-Aldrich HPA006983); anti-TRAF6 (Sigma-Aldrich HPA020599); anti-β-tubulin (Sigma-Aldrich T5293); anti-rabbit IgG, HRP, and anti-mouse IgG, HRP (Cell Signaling). Protein bands were visualized using the chemiluminescence detection kit Clarity Western ECL Substrate (Bio-Rad).

Results and Discussion

Proteomic profiling of EWS-FLI1 knockdown cells

EWS-ETS gene fusions are generally accepted as the major drivers of ES pathogenesis [23]. Given the function of the chimera protein as an aberrant transcription factor [9], the subsequent identification of EWS-FLI1 targets by proteomic approaches could be a key aspect in understanding the molecular behavior of ES. The alternative approach of inducing the ectopic expression of EWS-FLI1 in heterologous tumor cells did not always produce the desired effect, but rather in a wide variety of adverse effects, such as dedifferentiation or growth arrest [23]. So far, various proteomic approaches have been used to address biological issues in ES, including the study of disease mechanisms, molecular target identification, and biomarker development, though we are now only beginning to recognize their benefits [24-26].

In order to identify proteins associated with changes induced by EWS-FLI1 we compared the TC-71 cell line with a downregulated shEWS-FLI1 clone showing the most pronounced decrease in EWS-FLI1 expression [19]. Two-dimensional gel electrophoresis (2D-PAGE) analyses of 6 shEWS-FLI1 extracts and 6 control (pSUPER empty vector) from independent replicates were performed over a pH range of 3-11. Overall, images of 2-D gels showed similar distribution of proteins (Figure 1A). The digital analysis of the images detected changes in protein abundance levels for more than 500 spots in a virtual gel master. A pattern of more than 400 spots with identical positions was found on every gel replicate of each group. Forty-six spots were analyzed as being differentially abundant with significant changes of more than ± 1.8 folds ($p<0.05$). Of these spots, 43 proteins were successfully identified by MS, as summarized in Table 1. Among them, 25 proteins were overabundant in the shEWS-FLI1 model, whereas 14 proteins were highly abundant in the control cells.

Dependency on DNA/RNA processing proteins is revealed by GO analysis

The molecular functions and cellular localization of the proteins identified in the analysis was performed using GO as shown in Figure 2A. Interestingly, many of the identified proteins with the highest scores were molecules directly involved in DNA/RNA functioning and regulation, which makes sense in the context of the role played by the chimeric protein EWS-FLI1 in ES as an aberrant transcription factor. Next, we displayed the relative distribution of proteins in selected GO terms by their molecular function (Figure 2B). The first striking observation was the high number of proteins implicated in DNA and RNA processing. More than 15 molecular functions related to RNA processing were described for the proteins overrepresented in the shEWS-FLI1 dataset. In particular, there were at least 7 proteins bearing significant annotations in ribonucleoprotein complexes (nucleophosmin, different helicases, ribosomal proteins), and several proteins with helicase activity were described as altered in the shEWS-FLI1 model (DDX5, DDX39B, RUVBL2). The analysis also suggested that another 3 proteins were involved in DNA replication-associated processes (like proteins of proliferation, and proteasome components).

RUVBL2 is a component of both the RNA polymerase II holoenzyme complex (and therefore is involved in DNA recombination, DNA repair, and protein folding) and of the NuA4 histone acetyltransferase complex (involved in transcriptional activation of specific genes) [27]. When modified, it promote interaction of the histones H4 and H2A with transcription regulators, which will activate transcriptional programs associated with oncogene and proto-oncogene mediated growth induction, tumor suppressor mediated growth arrest and replicative senescence, apoptosis, and DNA repair. In addition, several histones (histone H2B type-1B, histone H2B type-1C, histone H2B type 2-F, and histone H3.3) were differentially overabundant in the interfered model. This suggests that EWS-FLI1 may play a role in DNA accessibility and that ES cells exhibit an activated cell-dividing activity, according to its tumorigenic capability. Recent reports have furnished evidence of the role of the chimera in the regulation of epigenome and transcriptome rewiring [28].

Similarly to RNA helicase A, which has been already described in ES [29], we found helicases of the DEAD box protein family, as well as helicases DDX5 and DDX39B, all of which may stimulate the transcriptional activity of EWS-FLI1 target gene promoters by directly

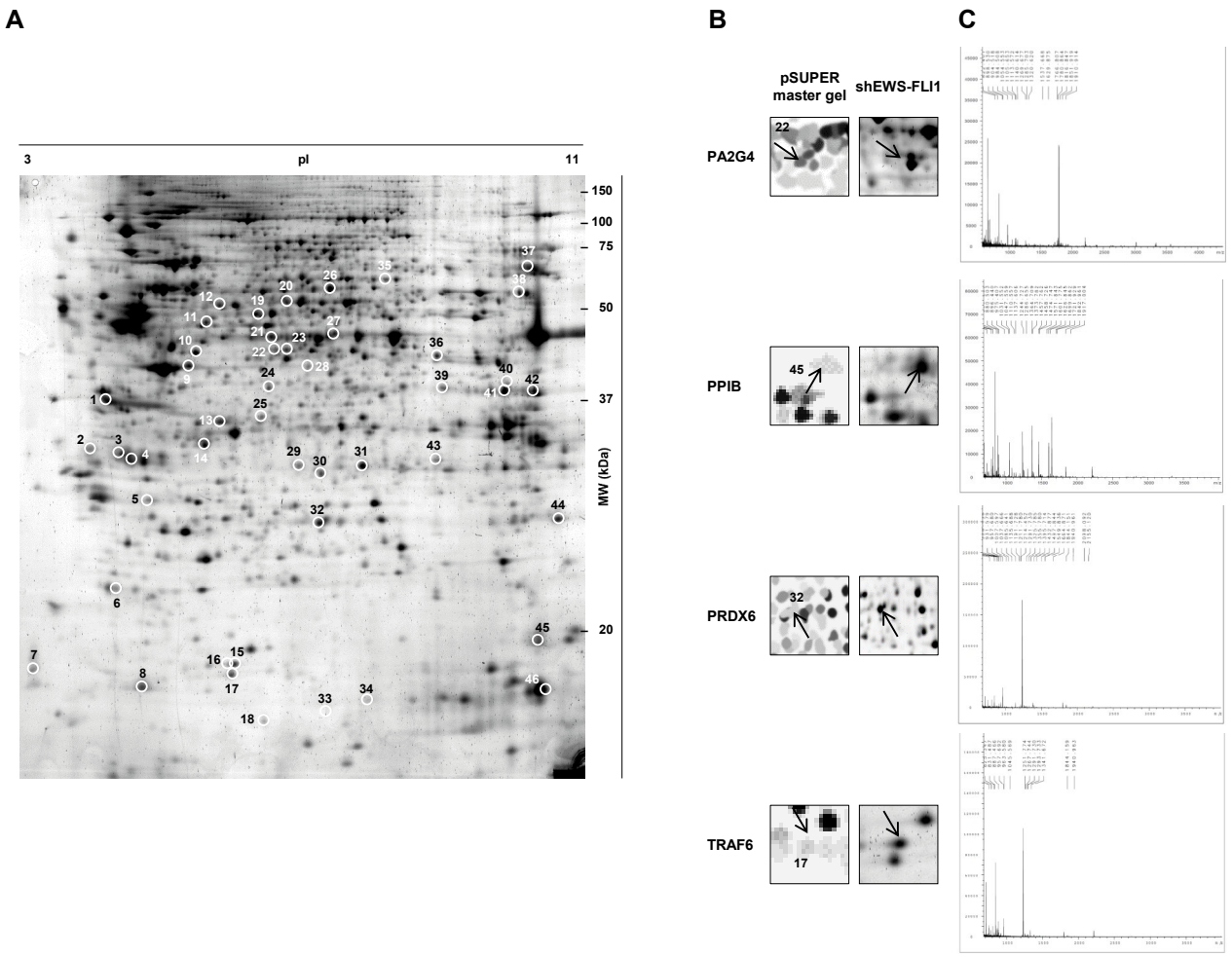

Figure 1: A) Representative 2-DE map of the proteome obtained from TC-71 cell line with shRNAi interference for EWS-FLI1. Differentially abundant spots that were subsequently analyzed by MS are marked with numbered circles. B) 2-DE images for PA2G4, PPIB, PRDX6, and TRAF6 proteins. Arrowheads indicate spots that were excised for MS analysis. Numbers indicate spot numbers as in panel A. C) MALDI-ToF mass spectra of tryptic digests of PA2G4, PPIB, PRDX6, and TRAF6.

Protein	UniProtKB/Swiss-Prot accession	Accession	Gene name	Spot no.	Abundance level variation	P value	Mass (kDa)	pI	MASCOT score
Translationally-controlled tumor protein	P13693	TCTP_HUMAN	TPT1	6	↑ 6,42	0.040	19.7	4.8	81
FSD1-like protein	Q9BXM9	FSD1L_HUMAN	FSD1L	8	↑ 6,61	0.009	17.0	5.9	89
Creatine kinase B-type	P12277	KCRB_HUMAN	CKB	9	↑ 4,73	0.005	42.9	5.4	115
RuvB-like 2	Q9Y230	RUVB2_HUMAN	RUVBL2	11	↑ 2,01	0.042	51.2	5.5	134
Spliceosome RNA helicase DDX39B	Q13838	DX39B_HUMAN	BAT1	11	↑ 2,01	0.042	49.4	5.4	125
Inorganic pyrophosphatase	Q15181	IPYR_HUMAN	PPA1	14	↑ 7,12	0.019	33.1	5.5	118
TNF receptor-associated factor 6	Q9Y4K3	TRAF6_HUMAN	TRAF6	17	↑ 5,70	0.023	61.2	6.0	48
Histone H2B type 1-B	P33778	H2B1B_HUMAN	HIST1H2BB	18	↑ 5,22	0.018	13.8	10.3	132
Tryptophan--tRNA ligase. cytoplasmic	P23381	SYWC_HUMAN	WARS	19	↑ 2,30	0.021	53.5	5.8	203
Rab GDP dissociation inhibitor beta	P50395	GDIB_HUMAN	GDI2	21	↑ 1,88	0.029	51.1	6.1	89
Dimethylaniline monooxygenase 2	Q99518	FMO2_HUMAN	FMO2	24	↑ 2,23	0.044	61.4	6.9	49
T-complex protein 1 subunit zeta	P40227	TCPZ_HUMAN	CCT6A	26	↑ 6,34	0.002	58.3	6.3	114

Delta(3.5)-Delta(2.4)-dienoyl-CoA isomerase. mitochondrial	Q13011	ECH1_HUMAN	ECH1	29	↑ 4,95	0.002	36.1	6.0	173
Peroxiredoxin-6	P30041	PRDX6_HUMAN	PRDX6	32	↑ 6,24	0.006	25.0	6.0	139
Histone H2B type 1-C/E/F/G/I	P62807	H2B1C_HUMAN	HIST1H2BC	33	↑ 5,72	0.008	13.7	10.3	116
Histone H3.3	P84243	H33_HUMAN	H3F3A	33	↑ 5,72	0.008	15.3	11.3	108
Histone H2B type 2-F	Q5QNW6	H2B2F_HUMAN	HIST2H2BF	34	↑ 4,76	0.010	13.8	10.3	93
Histone H3.3	P84243	H33_HUMAN	H3F3A	34	↑ 4,76	0.010	15.3	11.3	94
Citrate synthase. mitochondrial	O75390	CISY_HUMAN	CS	36	↑ 4,33	0.011	51.9	7.4	91
Probable ATP-dependent RNA helicase DDX5	P17844	DDX5_HUMAN	DDX5	37	↑ 7,01	0.002	69.6	9.1	109
Transcription initiation factor TFIID subunit 6	P49848	TAF6_HUMAN	TAF6	38	↑ 4,04	0.038	73.3	8.8	56
Fructose-bisphosphate aldolase A	P04075	ALDOA_HUMAN	ALDOA	41	↑ 2,77	0.050	39.7	8.4	132
PCI domain-containing protein 2	Q5JVF3	PCID2_HUMAN	PCID2	42	↑ 3,02	0.004	46.6	8.8	76
Cysteine-rich protein 2	P52943	CRIP2_HUMAN	CRIP2	44	↑ 3,45	0.018	23.3	9.0	90
Peptidyl-prolyl cis-trans isomerase B	P23284	PPIB_HUMAN	PPIB	45	↑ 2,90	0.004	22.8	9.3	313
Nucleophosmin	P06748	NPM_HUMAN	NPM1	1	↓ 5,05	0.001	32.7	4.6	188
Proliferating cell nuclear antigen	P12004	PCNA_HUMAN	PCNA	2	↓ 8,77	0.001	29.1	4.6	175
Proteasome subunit alpha type-3	P25788	PSA3_HUMAN	PSMA3	5	↓ 6,64	0.003	28.5	5.2	226
Protein disulfide-isomerase A3	P30101	PDIA3_HUMAN	PDIA3	12	↓ 7,06	0.002	57.1	5.6	187
V-type proton ATPase subunit B. brain isoform	P21281	VATB2_HUMAN	ATP6V1B2	12	↓ 7,06	0.002	56.8	5.6	182
60S acidic ribosomal protein P0	P05388	RLA0_HUMAN	RPLP0	13	↓ 6,51	0.004	34.4	5.7	228
T-complex protein 1 subunit beta	P78371	TCPB_HUMAN	CCT2	20	↓ 5,64	0.006	57.7	6.0	251
Proliferation-associated protein 2G4	Q9UQ80	PA2G4_HUMAN	PA2G4	22	↓ 6,37	0.029	44.0	6.1	261
Proliferation-associated protein 2G4	Q9UQ80	PA2G4_HUMAN	PA2G4	23	↓ 5,63	0.001	44.0	6.1	99
Serine/threonine-protein phosphatase PP1-beta catalytic subunit	P62140	PP1B_HUMAN	PPP1CB	25	↓ 6,95	0.001	37.8	5.9	204
Alpha-enolase	P06733	ENOA_HUMAN	ENO1	27	↓ 5,33	0.007	47.4	7.0	162
Septin-5	Q99719	SEPT5_HUMAN	SEPT5	28	↓ 5,16	0.024	43.2	6.2	133
S-formylglutathione hydrolase	P10768	ESTD_HUMAN	ESD	31	↓ 6,42	0.000	32.0	6.5	236
Heterogeneous nuclear ribonucleoprotein L	P14866	HNRPL_HUMAN	HNRPL	35	↓ 6,59	0.004	60.7	8.5	180
Phosphoserine aminotransferase	Q9Y617	SERC_HUMAN	PSAT1	39	↓ 7,70	0.002	40.8	7.6	301
Sorbitol dehydrogenase	Q00796	DHSO_HUMAN	SORD	40	↓ 8,43	0.002	38.8	8.3	272
Voltage-dependent anion-selective channel protein 2	P45880	VDAC2_HUMAN	VDAC2	43	↓ 5,89	0.003	38.6	7.7	187
Fibroblast growth factor 2	P09038	FGF2_HUMAN	FGF2	46	↓ 8,58	0.030	17.5	9.6	48

Table 1: List of 43 unique proteins identified as differentially abundant in ES TC-71 cells, as a result of the inhibition of EWS-FLI1 fusion by shRNAi. They included proteins with at least 1.8-fold increased abundance levels in shEWS-FLI1 model and proteins with at least 1.8-fold decreased abundance levels. P values measure the significance of the difference between proteins from shEWS-FLI1 gels and proteins from control gels, calculated by an independent-samples T-test for each spot. Spot numbers correspond to those in Figure 1.

interacting with EWS-FLI1. In fact, a recent study has confirmed the relevance of EWS-FLI1 as a network hub that modulates systemic alternative splicing as an oncogenic process [30]. Similarly, hnRNP L, PCNA, and TAF70 are components of several nuclear complexes that play a central role in mediating promoter responses to various activators and repressors [31]. These factors show changes in their expression levels, and it is suspected that some of them bear activating and deactivating signals in their posttranslational modification patterns, as a result of EWS-FLI1 induction in ES cells [25]. Proteins related to the translational programme were also altered. This is the

Citation: Madoz-Gúrpide J, Herrero-Martín D, Gómez-López G, Hontecillas-Prieto L, Biscuola M, et al. (2016) Proteomic Profiling of Ewing Sarcoma Reveals a Role for TRAF6 in Proliferation and Ribonucleoproteins/RNA Processing. J Proteomics Bioinform 9: 166-175. doi:10.4172/jpb.1000403

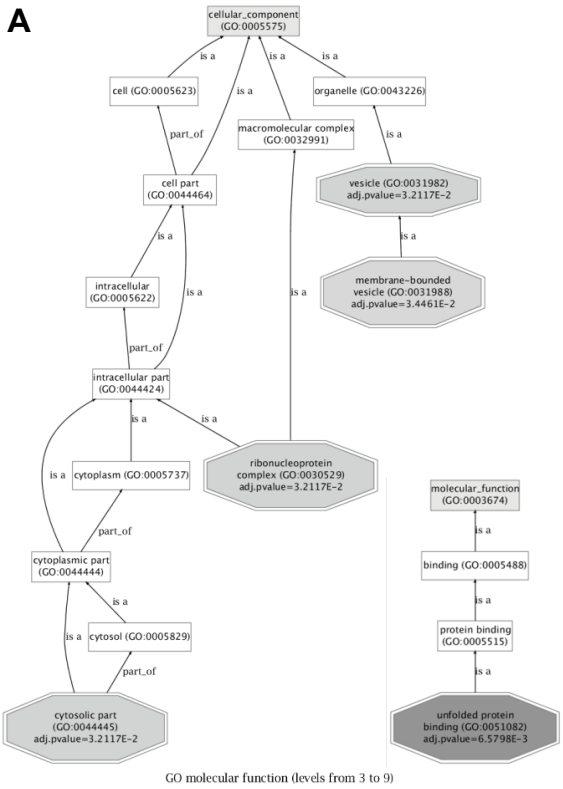

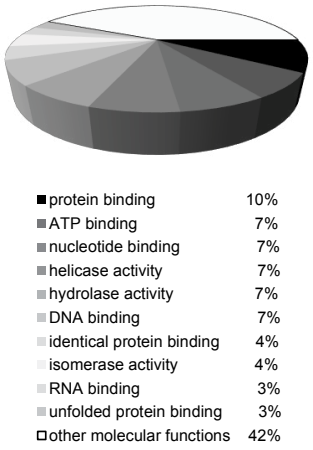

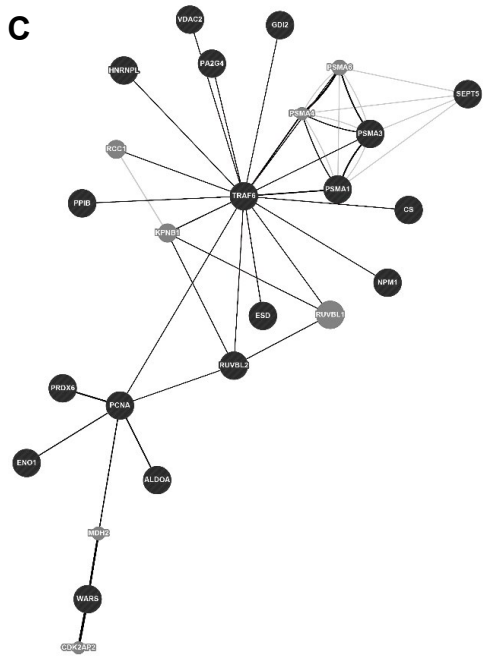

Figure 2: GO annotation of the proteins altered in our shEWS-FLI1 TC-71 cell line model, as listed in Table 1. A) Graphic network of the significantly enriched GO categories (FDR<0.05) for cellular components and molecular function. The gray-colored gradient is directly proportional to the significance, from white (non-significant) to black (most). B) Relative distribution of proteins in selected GO terms by their molecular function. C) Pathway analysis report showing the interactions between the proteins altered in TC-71 cells by shEWS-FLI1. A GeneMANIA-generated network seeded with the proteins specific to EWS-FLI1 knocking-down (Table 1), pointing out TRAF6 as a hub node. The predictions of GeneMANIA were based on co-expression, co-localization, genetic interactions, pathways, physical interactions, predicted interactions, and shared protein domains. Protein queries–selected from our analysis–are black-filled circles. Other network proteins are gray-filled circles. Black lines correspond to physical interactions, while grey lines represent pathways.

case of nucleophosmin, which has already been proposed as a candidate independent prognostic marker for ES patients, as identified by another proteomic approach [26]. Taken together, all these alterations reflect direct consequences of an aberrant transcriptional activity of the chimera protein.

Cell-cycle proteins involved in the growth of tumors are overabundant in ES cells

Another group of proteins altered in TC-71 cells are associated with cell cycle and cell division activities. One of these is PA2G4, whose abundance level is reduced in the shEWS-FLI1 silenced cells (Figure 1B). This result is consistent with the data from the gene expression microarray study of this clone (PA2G4 score value = -6.62) [19]. PA2G4 forms part of a ribonucleoprotein complex that acts as a negative regulator of transcription, and may be involved in regulation of rRNA processing, either directly or through an E2F switch. Additionally, PA2G4 may also play a role in erbB-3-regulated signal transduction pathway. Interestingly, erbB-3expression levels have been reported to be typically upregulated in pediatric alveolar rhabdomyosarcoma [32]. Since ES proteins share the same N-terminal EWS domain, PA2G4 overabundance may reflect changes in erbB-3 levels and in its downstream transcriptional activation pathways. This point merits further confirmation.

Another protein involved in cell-cycle is PP1B, which is essential for cell division as it participates in the regulation of glycogen metabolism and protein synthesis. PP1B decreased its protein abundance levels in the EWS-FLI1 knockdown cells (Figure 1B), in agreement with previous reports that elucidate its role in malignant bone and soft tissue tumors [33]. From IHC analysis, it was proven that the percentage of cells stained positively with antiserum against PP1B was significantly higher in ES than in benign tumors. Furthermore, the malignant tumor lesions showed a markedly high number of cells in the S-phase fraction of the cell cycle, as compared to benign tumors. Taken together, these results suggest that PP1B is involved in the accelerated growth of malignant tumor cells.

Finally, PSA3, a component of the proteasome, and septin-5 are more abundant in TC-71 tumor cells. Differential levels of both proteins have been associated with several tumor types.

Changes in protein abundance related to metabolism reprogramming

The analysis of overrepresentation confirmed the previous findings and revealed a pattern of metabolic changes in the shEWS-FLI1 model. Since the mid-1950s, it has been well-known that cancer cells adjust their energy metabolism in order to fuel cell growth and division [34], and many genes have been related to this switch during recent decades. In our study, TC-71 cells exhibited abundant levels of alpha-enolase (ENOA). This is a multifunctional enzyme that is upregulated in cancers of the cartilage or bone marrow (among others), and that has been proposed as being of diagnostic and prognostic value [35]. Although some attention has been devoted to the role of metabolism in other pediatric sarcomas (rhabdomyosarcoma for instance) [36], this is one of the few studies reporting about metabolism in ES.

Other proteins in the EWS-FLI1-downregulated cells are engaged in protein binding, folding, rearranging of polypeptidic structures, or even modulation of p53-dependent functions (PPIB, PDIA3, TCPB). High levels of these proteins may provide some clues about the molecular changes accompanying the redifferentiation program of cells after impairment of the fusion protein expression.

TRAF6 is a hub connecting multiple targets

Notably, many of the proteins listed in Table 1 are described in the overrepresentation analysis as showing direct physical interactions among each other. Among them, TRAF6 (TNF receptor-associated factor 6) appears as a hub node, highly connected to several other proteins on the list (Figure 2C). Given that TRAF-family proteins are associated with, and mediate, signal transduction from various signaling pathways, the high number and functional heterogeneity of the TRAF6 counterparts found in our analysis (isomerases, proteasome subunits, Rab GDP dissociation inhibitor, citrate synthase, etc.) are unsurprising. It also provides a link between distinct signaling pathways, as it interacts with various protein kinases (IRAK1/IRAK, SRC, and PKCzeta). Similarly, it has been linked to the incorrect regulation of NF-kappaB as well as to alterations in JNK and p38 signaling pathways In consequence, TRAF6 upregulation in the absence of EWS-FLI1 would fit in the context of regulatory changes in the abundance levels of signaling proteins leading to tumorigenic processes.

Finally, the search for enrichment in miRNA targets uncovered miR-363 as a potential regulatory candidate for 7 proteins within our list (FDR<0.05): 4 targets were upregulated in the control cells, whereas 3 proteins were increased in the shEWS-FLI1 cells. It is generally accepted that miR-363 functions in many cancer types as an oncomiR. Recent studies have identified upregulation of miR-106a~363 cluster in ES, and provide support for a pro-oncogenic role of this microRNA cluster [37]. In numerous ES cell lines, however, and according to our own miRNA profiling research, miR-363 basal expression levels are usually low (including TC-71 cell line), and they barely change when the EWS-FLI1 protein fusion is silenced (unpublished data). In our proteomic study, the enrichment for miR-363 targets was significant (7/44 proteins), with 3 of the target proteins upregulated in the silenced cells and 4 in the TC-71 cells. It is clear that some other miRNA must be playing a role in the regulation of these protein alterations following EWS-FLI1 knocking-down. In consequence, from the integration of this whole body of data, we cannot provide conclusive information on the nature of the modulation of miR-363 in response to EWS-FLI1 knockdown in the TC-71 ES cell line.

Validation of abundance levels of selected candidates in ES cell lines

We selected 4 proteins from Table 1 for which abundance levels were analyzed in several ES cell lines as well as in samples from patients: TRAF6 (as a hub node connected to other proteins on the list); PRDX6 (participating in metabolic pathways); PPIB (accelerates the folding of proteins by binding to peptides and RNA polymerase, ultimately contributing to bone development); and PA2G4 (a RNA processing protein that interacts with erbB3). PA2G4 is more abundant in the TC-71 cell line, whereas PPIB, PRDX6, and TRAF6 increase their levels when the chimera protein is silenced.

We initially characterized the gene expression levels of these proteins by quantitatively analyzing their corresponding mRNA levels across a panel of 15 ES cell lines (Figure 3A). Data were normalized with respect to the levels of the IMR90 fibroblast line, and hMSC (human mesenchymal stem cells) were used as controls for comparison of levels. qPCR results showed different trends in the patterns of expression for the assayed genes, i.e., more or less expressed in the ES cells than in the controls, although the results were homogeneous in the 4 scenarios: 85% of the cell lines showed similar mRNA levels for a given gene. PA2G4 levels were consistently elevated (FC>3.0) in the tumor cells as well as in the hMSC. On the other hand, PPIB levels were decreased in all the

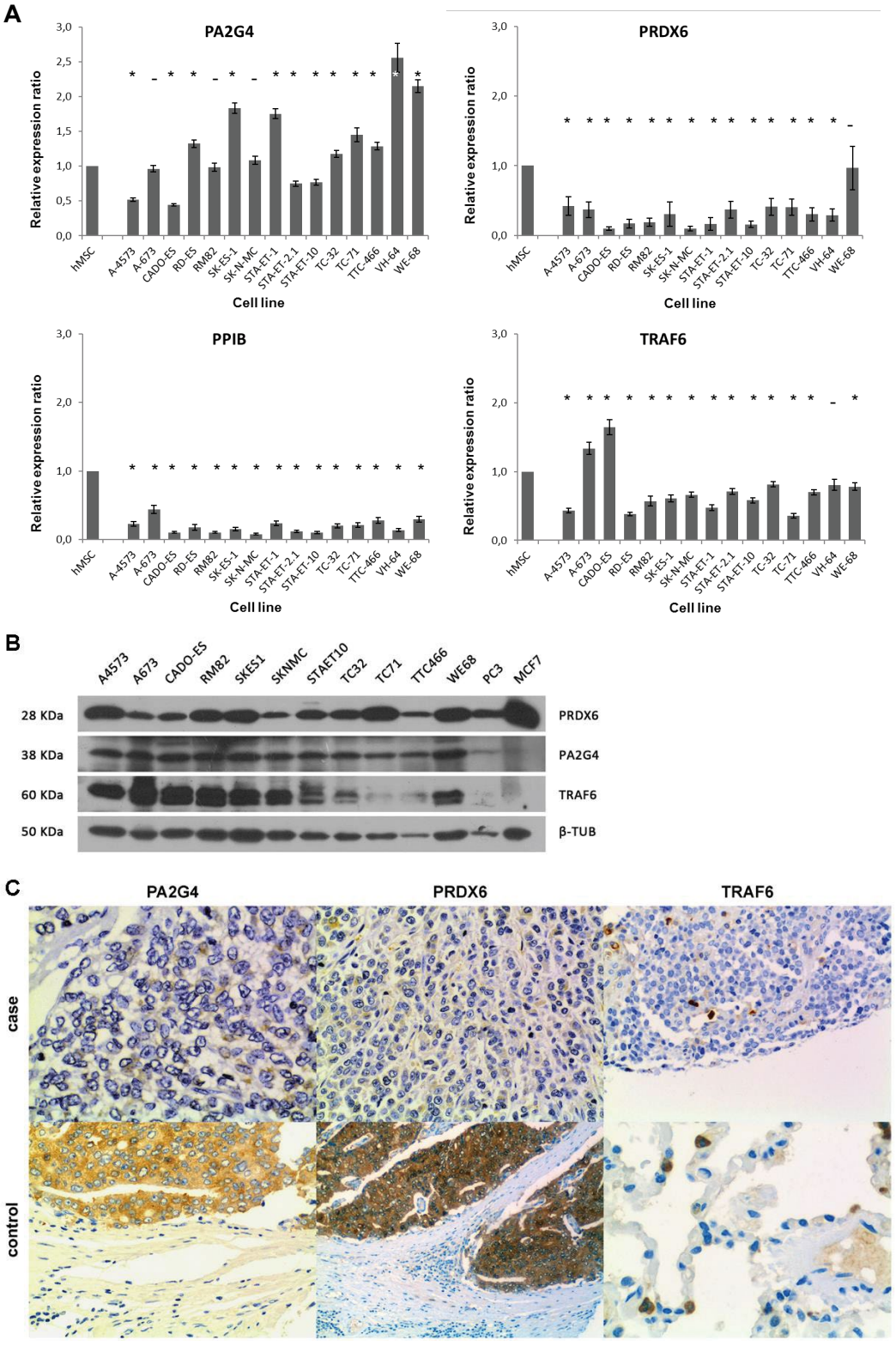

Figure 3: Assessment of PA2G4, PPIB, PRDX6, and TRAF6 levels. A) mRNA expression levels for selected target genes were determined by qPCR analysis in 15 ES cell lines and in hMSC control line. Experiments were repeated three times. *: P<0.05. B) Total protein extract levels were assayed by WB for PA2G4, PRDX6, and TRAF6 abundance measurement in 11 ES cell lines. Two additional cell lines (MCF7, breast; PC-3, prostate) were included as controls. C) Representative images of ES cases and non-ES controls obtained by IHC with PA2G4, PRDX6, and TRAF6 antibodies in tissue microarray sections.

cell lines with respect to both the fibroblasts and the hMSC. Meanwhile, most of the cell lines displayed TRAF6 and PRDX6 expression levels similar to the controls. For PA2G4, PRDX6, and TRAF6, mRNA levels were 2-3 times higher in hMSC than in IMR90.

In general, protein abundance levels, as estimated by WB analysis, revealed a similar pattern. PA2G4 levels were homogeneous in a panel of 11 ES cell lines (plus 2 additional prostate and breast cancer lines, used as controls, Figure 3B), with moderately superior abundance levels as compared to the controls. PRDX6 protein levels varied from cell line to line with 2-3 fold differences, and all cases were between levels for prostate and breast cancer cells. TRAF6 was abundant in most ES cell lines, but apparently not in the controls. If we take a closer look at the TC-71 cell line, from which the shRNA model was constructed, we can observe that TRAF6 levels were low, in accordance with 2-D PAGE results (Figure 1B). Most of the other cell lines exhibited higher abundance levels for TRAF6.

ES tumor samples show low levels of selected proteins by IHC

PA2G4, PRDX6, and TRAF6 antibodies gave consistent signals in 3 different ES TMAs, for a total number of 42 ES samples (Figure 3C). A pattern of sample heterogeneity was visualized in the IHC analysis of the PA2G4 protein. The signal for PA2G4 was ubiquitously cytoplasmic, but the extent of abundance in tumor samples was unexpectedly low, with 2% of positive cases. On the contrary, tumor cells were not supposed to express either PRDX6 or TRAF6, and the IHC results confirmed that issue (5% of cases staining for PRDX6 and 0% for TRAF6). In both cases, staining was also cytoplasmic, as seen in the control samples (pancreas, epididymis, prostate, prostate carcinoma, breast, breast carcinoma). The signal for TRAF6 was also visualized in the surrounding inflammatory cells but not in the tumor cells.

Concluding Remarks

In spite of the significant progress made over recent years in describing the molecular biology of ES, it remains a largely unknown disease in many key points of its pathogenesis. A combination of EWS-FLI1 chimera silencing, 2-DE/mass spectrometry analysis, and ontology modeling have been employed to address this pathology. In summary, it has revealed that EWS-FLI1 modulates RNA processing and transcription regulation, and it might be involved in cell-cycle control and metabolism functioning. This study confirmed the value of proteomic approaches to uncover complex regulatory mechanisms unleashed by the aberrant behavior of a key transcription factor. Under this assumption, our work is a valuable example for gaining knowledge to the role of EWS-FLI1 as an epitome of fusions governing the pathogenesis of sarcomas.

Acknowledgements

The authors thank the donors and the HUVR-IBiS Biobank (Andalusian Public Health System Biobank and ISCIII-Red de Biobancos PT13/0010/0056) for the human specimens used in this study. Research in EA's lab is supported by the Ministry of Science and Innovation of Spain-FEDER (PI1401466, PI081828, RD06/0020/0059, RD12/0036/0017).

Conflict of Interest

The authors have declared no conflict of interest.

Author Contributions

Conceived and designed the experiments: Juan Madoz-Gúrpide, Enrique de Álava. Performed the experiments: Juan Madoz-Gúrpide, David Herrero-Martín, Lourdes Hontecillas-Prieto, Cristina Chamizo. Analyzed the data: Juan Madoz-Gúrpide, Gonzalo Gómez-López. Contributed reagents/materials/analysis tools: Juan Madoz-Gúrpide, David Herrero-Martín, Michele Biscuola, Gonzalo Gómez-López, Enrique de Álava. Wrote the paper: Juan Madoz-Gúrpide.

References

1. Rodriguez-Galindo C, Spunt SL, Pappo AS (2003) Treatment of Ewing sarcoma family of tumors: current status and outlook for the future. Med Pediatr Oncol 40: 276-287.
2. Esiashvili N, Goodman M, Marcus RB Jr (2008) Changes in incidence and survival of Ewing sarcoma patients over the past 3 decades: Surveillance Epidemiology and End Results data. J Pediatr Hematol Oncol 30: 425-430.
3. Gaspar N, Hawkins DS, Dirksen U, Lewis IJ, Ferrari S, et al. (2015) Ewing Sarcoma: Current Management and Future Approaches Through Collaboration. J Clin Oncol 33: 3036-3046.
4. Gorlick R, Janeway K, Lessnick S, Randall RL, Marina N; COG Bone Tumor Committee (2013) Children's Oncology Group's 2013 blueprint for research: bone tumors. Pediatr Blood Cancer 60: 1009-1015.
5. Delattre O, Zucman J, Plougastel B, Desmaze C, Melot T, et al. (1992) Gene fusion with an ETS DNA-binding domain caused by chromosome translocation in human tumours. Nature 359: 162-165.
6. Sorensen PH, Lessnick SL, Lopez-Terrada D, Liu XF, Triche TJ, et al. (1994) A second Ewing's sarcoma translocation, t(21;22), fuses the EWS gene to another ETS-family transcription factor, ERG. Nat Genet 6: 146-151.
7. May WA, Arvand A, Thompson AD, Braun BS, Wright M, et al. (1997) EWS/FLI1-induced manic fringe renders NIH 3T3 cells tumorigenic. Nat Genet 17: 495-497.
8. Mackintosh C, Madoz-Gúrpide J, Ordóñez JL, Osuna D, Herrero-Martín D (2010) The molecular pathogenesis of Ewing's sarcoma. Cancer Biol Ther 9: 655-667.
9. Prieur A, Tirode F, Cohen P, Delattre O (2004) EWS/FLI-1 silencing and gene profiling of Ewing cells reveal downstream oncogenic pathways and a crucial role for repression of insulin-like growth factor binding protein 3. Mol Cell Biol 24: 7275-7283.
10. Dauphinot L, De Oliveira C, Melot T, Sevenet N, Thomas V, et al. (2001) Analysis of the expression of cell cycle regulators in Ewing cell lines: EWS-FLI-1 modulates p57KIP2and c-Myc expression. Oncogene 20: 3258-3265.
11. Amsellem V, Kryszke MH, Hervy M, Subra F, Athman R, et al. (2005) The actin cytoskeleton-associated protein zyxin acts as a tumor suppressor in Ewing tumor cells. Exp Cell Res 304: 443-456.
12. Mendiola M, Carrillo J, García E, Lalli E, Hernández T, et al. (2006) The orphan nuclear receptor DAX1 is up-regulated by the EWS/FLI1 oncoprotein and is highly expressed in Ewing tumors. Int J Cancer 118: 1381-1389.
13. Thompson AD, Teitell MA, Arvand A, Denny CT (1999) Divergent Ewing's sarcoma EWS/ETS fusions confer a common tumorigenic phenotype on NIH3T3 cells. Oncogene 18: 5506-5513.
14. Deneen B, Denny CT (2001) Loss of p16 pathways stabilizes EWS/FLI1 expression and complements EWS/FLI1 mediated transformation. Oncogene 20: 6731-6741.
15. Lessnick SL, Dacwag CS, Golub TR (2002) The Ewing's sarcoma oncoprotein EWS/FLI induces a p53-dependent growth arrest in primary human fibroblasts. Cancer Cell 1: 393-401.
16. Zwerner JP, Guimbellot J, May WA (2003) EWS/FLI function varies in different cellular backgrounds. Exp Cell Res 290: 414-419.
17. Hancock JD, Lessnick SL (2008) A transcriptional profiling meta-analysis reveals a core EWS-FLI gene expression signature. Cell Cycle 7: 250-256.
18. Chen G, Gharib TG, Huang CC, Taylor JM, Misek DE, et al. (2002) Discordant protein and mRNA expression in lung adenocarcinomas. Mol Cell Proteomics 1: 304-313.
19. Herrero-Martín D, Osuna D, Ordóñez JL, Sevillano V, Martins AS, et al. (2009) Stable interference of EWS-FLI1 in an Ewing sarcoma cell line impairs IGF-1/IGF-1R signalling and reveals TOPK as a new target. Br J Cancer 101: 80-90.
20. Martins AS, Mackintosh C, Martín DH, Campos M, Hernández T, et al. (2006) Insulin-like growth factor I receptor pathway inhibition by ADW7, alone or in combination with imatinib, doxorubicin, or vincristine, is a novel therapeutic approach in Ewing tumor. Clin Cancer Res 12: 3532-3540.
21. Käll L , Canterbury JD, Weston J, Noble WS, MacCoss MJ (2007) Semi-supervised learning for peptide identification from shotgun proteomics datasets. Nat Methods 4: 923-925.

22. Medina I, Carbonell J, Pulido L, Madeira SC, Goetz S, et al. (2010) Babelomics: an integrative platform for the analysis of transcriptomics, proteomics and genomic data with advanced functional profiling. Nucleic Acids Res 38: W210-W213.

23. Kovar H (2005) Context matters: the hen or egg problem in Ewing's sarcoma. Semin Cancer Biol 15: 189-196.

24. Guipaud O, Guillonneau F, Labas V, Praseuth D, Rossier J, et al. (2006) An in vitro enzymatic assay coupled to proteomics analysis reveals a new DNA processing activity for Ewing sarcoma and TAF(II)68 proteins. Proteomics 6: 5962-5972.

25. Pahlich S, Quero L, Roschitzki B, Leemann-Zakaryan RP, Gehring H (2009) Analysis of Ewing sarcoma (EWS)-binding proteins: interaction with hnRNP M, U, and RNA-helicases p68/72 within protein-RNA complexes. J Proteome Res 8: 4455-4465.

26. Kikuta K, Tochigi N, Shimoda T, Yabe H, Morioka H, et al. (2009) Nucleophosmin as a candidate prognostic biomarker of Ewing's sarcoma revealed by proteomics. Clin Cancer Res 15: 2885-2894.

27. Doyon Y, Selleck W, Lane WS, Tan S, Côté J (2004) Structural and functional conservation of the NuA4 histone acetyltransferase complex from yeast to humans. Mol Cell Biol 24: 1884-1896.

28. Tomazou EM, Sheffield NC, Schmidl C, Schuster M, Schönegger A, et al. (2015) Epigenome mapping reveals distinct modes of gene regulation and widespread enhancer reprogramming by the oncogenic fusion protein EWS-FLI1. Cell Reports 10: 1082-1095.

29. Erkizan HV, Schneider JA, Sajwan K, Graham GT, Griffin B, et al. (2015) RNA helicase A activity is inhibited by oncogenic transcription factor EWS-FLI1. Nucleic Acids Res 43: 1069-1080.

30. Selvanathan SP, Graham GT, Erkizan HV, Dirksen U, Natarajan TG, et al. (2015) Oncogenic fusion protein EWS-FLI1 is a network hub that regulates alternative splicing. Proc Natl Acad Sci U S A 112: E1307-E1316.

31. Weinzierl RO, Ruppert S, Dynlacht BD, Tanese N, Tjian R (1993) Cloning and expression of Drosophila TAFII60 and human TAFII70 reveal conserved interactions with other subunits of TFIID. EMBO J 12: 5303-5309.

32. Nordberg J, Mpindi JP, Iljin K, Pulliainen AT, Kallajoki M, et al. (2012) Systemic analysis of gene expression profiles identifies ErbB3 as a potential drug target in pediatric alveolar rhabdomyosarcoma. PLoS One 7: e50819.

33. Sogawa K, Yamada T, Sugita A, Kito K, Tachibana M, et al. (1996) Role of protein phosphatase in malignant osteogenic and soft tissue tumors. Res Commun Mol Pathol Pharmacol 93: 33-42.

34. Warburg O (1956) On respiratory impairment in cancer cells. Science 124: 269-270.

35. Capello M, Ferri-Borgogno S, Cappello P, Novelli F (2011) α-Enolase: a promising therapeutic and diagnostic tumor target. FEBS J 278: 1064-1074.

36. Monti E, Fanzani A (2016) Uncovering metabolism in rhabdomyosarcoma. Cell Cycle 15: 184-195.

37. Dylla L, Jedlicka P (2013) Growth-Promoting Role of the miR-106a approximately 363 Cluster in Ewing Sarcoma. PLoS One 8: e63032.